

1 **Fatty Liver and Impaired Hepatic Metabolism Alters the Congener-**
2 **specific Distribution of**
3 **Polychlorinated Biphenyls (PCBs) in Mice with A Liver-specific**
4 **Deletion of Cytochrome P450 Reductase**

5
6 *Xueshu Li, Chunyun Zhang, Hans-Joachim Lehmler**

7 Department of Occupational and Environmental Health, University of Iowa, Iowa City, IA 52242, USA

8
9
10
11
12
13
14
15 Corresponding Author:

16 Dr. Hans-Joachim Lehmler

17 The University of Iowa

18 Department of Occupational and Environmental Health

19 University of Iowa Research Park, #221 IREH

20 Iowa City, IA 52242-5000

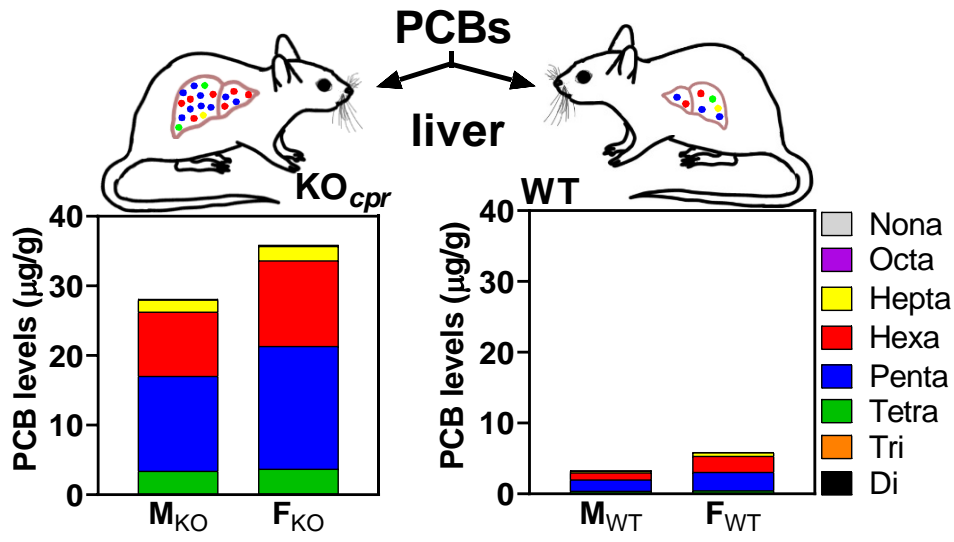
21 Phone: (319) 335-4981

22 Fax: (319) 335-4290

23 e-mail: hans-joachim-lehmler@uiowa.edu

24 ABSTRACT

25 Polychlorinated biphenyls (PCBs) are persistent organic pollutants that are linked to adverse
26 health outcomes. PCB tissue levels are determinants of PCB toxicity; however, it is unclear how factors,
27 such as an altered metabolism and/or a fatty liver, affect PCB distribution *in vivo*. We determined the
28 congener-specific disposition of PCBs in mice with a liver specific deletion of cytochrome P450
29 reductase (KO), a model of fatty liver with impaired hepatic metabolism, and wildtype (WT) mice. Male
30 and female KO and WT mice were exposed orally to Aroclor 1254, a technical PCB mixture. PCBs were
31 quantified in adipose, blood, brain and liver tissues by gas chromatography-mass spectrometry. PCB
32 profiles and levels in tissues were genotype and sex dependent. PCB levels were higher in the liver from
33 KO compared to WT mice. PCB profiles showed clear differences between tissues from the same
34 exposure group. While experimental tissue : blood partition coefficients in KO and WT mice did not
35 follow the trends predicted using a composition-based model, the agreement between experimental and
36 calculated partition coefficients was still reasonable. Thus, a fatty liver and/or an impaired hepatic
37 metabolism alter the distribution of PCBs in mice and the magnitude of the partitioning of PCBs from
38 blood into tissues can be approximated using composition-based models.



40

41 INTRODUCTION

42 Exposure to polychlorinated biphenyls (PCBs), a group of 209 persistent organic pollutants, is
43 associated with adverse human health effects, including cancer, developmental neurotoxicity, and effects
44 on the immune system.¹ Humans are exposed to complex mixtures of >150 PCB congeners via the diet,
45 dermally or, as recent studies demonstrate, by inhalation.¹⁻⁴ In contrast, *in vitro* and *in vivo* studies of
46 PCBs typically employ individual congeners or simplified and technical PCB mixtures. The disposition
47 of individual PCBs in standard laboratory animals, especially after oral exposure, is well investigated.
48 Several more recent studies also report the tissue distribution of PCBs after inhalation exposure in rats.⁵⁻⁷
49 Toxicokinetic models have been developed for individual PCB congeners or simple PCB mixture in
50 rodent models following oral^{8,9} and intravenous exposure.^{10,11} These studies provide insights into the
51 levels of PCBs in target tissues, such as the adipose tissue, blood, liver, or brain, thus allowing the
52 translation of results from toxicity studies with PCBs to humans. As a rule of thumb, PCB levels are
53 directly proportional to the fat content of a tissue, and, in wildtype rodents, follow the general order
54 adipose > liver > brain > blood.¹²⁻¹⁴ However, the PCB disposition can differ from this general trend,
55 depending on the animal model, the experimental design or other factors.

56 Factors affecting PCB disposition include an altered (hepatic) metabolism and redistribution away
57 from the site of metabolism to tissues with high-fat content.^{10,15} The induction of hepatic cytochrome
58 P450 enzymes will more rapidly eliminate episodic and some persistent PCB congeners.¹⁶ In sub-chronic
59 studies, growth dilution can contribute to the distribution of PCBs.¹⁷ Also, changes in the composition of
60 body compartments can shift the distribution of PCBs. Starvation shifts the partitioning of PCB 153 from
61 adipose to other tissues.¹⁸ Similarly, PCB 153 is mobilized from fat tissues during lactation and
62 redistributed to the breast milk.¹⁹ Fatty liver caused by exposure to PCB 126 produces a redistribution of
63 PCBs from the adipose tissue to the liver.^{20,21} There is also evidence that transgenic animals, which are
64 powerful tools to study the toxicity of PCBs *in vivo*, can have a bodyweight or body composition that
65 differs from wildtype animals and, thus, can affect the disposition of PCBs. Multidrug resistance

66 transporter 1a/b knockout mice have a significantly higher body weight compared to congenic wildtype
67 animals, which significantly alters PCB tissue levels.¹³ Mice with a liver specific deletion of cytochrome
68 P450 reductase (KO mice), the obligate electron donor of cytochrome P450 enzymes, have much higher
69 levels of PCBs in the liver than congenic wildtype mice (WT mice) due to a higher hepatic fat and protein
70 content.^{22, 23}

71 The objective of the present study was to determine how a fatty liver and an impaired hepatic PCB
72 metabolism alters the congener-specific disposition of PCBs following exposure to a complex PCB
73 mixture. PCB congener profiles, levels, and tissue : blood ratios were determined in target tissues
74 (adipose tissue, blood, brain, and liver) after acute oral exposure of male and female KO and congenic
75 WT mice to Aroclor 1254, a technical PCB mixture. PCB profiles and, to some extent, PCB levels in
76 these tissues were genotype and sex-dependent and, at the time point investigated, showed clear
77 differences between tissues from the same exposure group. An acceptable agreement was observed
78 between the experimental tissue : blood partition coefficients of the PCB congeners included in the
79 analysis and partition coefficients calculated using a composition-based model. These results demonstrate
80 that a fatty liver and an impaired hepatic metabolism alter the distribution of PCBs in mice, but that the
81 partitioning of PCBs from blood into tissues can be approximated using composition-based models.

82 EXPERIMENTAL SECTION

83 **Chemicals and Reagents.** Aroclor 1254 (lot #: KB 05-612) was provided by Dr. Larry Hansen. A
84 detailed characterization of this Aroclor 1254 batch has been reported previously.²⁴ Analytical standard
85 solutions containing all 209 PCB congeners was purchased from AccuStandard (New Haven, CT, USA).
86 ¹³C₁₂-2,5-Dichlorobiphenyl (¹³C-PCB 9, purity 100%, ¹³C₁₂, 99%) and ¹³C₁₂-2,2',3,3',4,4',5,5'-
87 octachlorobiphenyl (¹³C-PCB 194, purity 98%, ¹³C₁₂, 98%) were obtained from Cambridge Isotope
88 Laboratories (Tewksbury, Massachusetts, USA). 2,4,6-Trichlorobiphenyl-2',3',4',5',6'-d₅ (d-PCB 30), and
89 2,3,5,6-tetrachlorobiphenyl-2',3',4',5',6'-d₅ (d-PCB 65) were purchased from CDN Isotopes (Pointe Claire,
90 Quebec, Canada). Florisil (60-100 mesh), diatomaceous earth (DE), pesticide grade solvents and stripped

91 corn oil (lot #: A0234007, product of BE) were purchased from Fisher Scientific (Fair Lawn, NJ, USA).
92 The PCB nomenclature used follows the EPA nomenclature.²⁵

93 **Mouse model maintenance.** Alb-Cre^{+/-}/Cpr^{lox+/-} mice with a liver-specific deletion of the cytochrome
94 P450 oxidoreductase (EC 1.6.2.4) gene (knockout, KO) and congenic Alb-Cre^{-/-}/Cpr^{lox+/-} mice (wildtype,
95 WT) were obtained from Dr. Xinxin Ding (University of Arizona, AZ, USA) to establish a breeding
96 colony at the University of Iowa.^{26, 27} The mouse colony was maintained as described previously.^{23, 28}
97 Briefly, animals were housed in standard plastic cages in a temperature- and humidity-controlled
98 environment (21–23 °C) with a 12h light-dark cycle. Water and Basal diet (Harlan 7913 with 18%
99 protein, 6% fat, and 5% fiber) were provided *ad libitum*. Compared with WT mice, the KO mice have a
100 fatty liver and do not display any CPR activity in liver.²³

101 **Animal exposure.** The Institutional Animal Care and Use Committee of the University of Iowa
102 approved all animal procedures (protocol #: 1206120). Daily animal welfare-assessments were performed
103 by laboratory personnel, and no adverse outcomes were observed throughout the study. Eight-week-old
104 mice were randomly divided into control and exposure groups and exposed to corn oil (10 mL/kg body
105 weight) alone or Aroclor 1254 (16 mg/kg body weight in corn oil, 10 mL/kg body weight), respectively.
106 The dose was selected based on a previous animal study.¹² The animals were euthanized 24 h after PCB
107 exposure. Whole blood was collected by cardiac puncture and stored at – 20 °C in glass tubes with 80 µL
108 of ethylenediaminetetraacetic acid solution (EDTA, 7.5% w/w).¹² Tissues (adipose tissue, brain, and liver)
109 were collected and stored at -80 °C.

110 **PCB extraction.** PCBs were extracted from adipose (0.05-0.09 g), brain (0.10-0.15), liver (0.06-0.18
111 g) and blood (0.55-0.73 g) with a pressurized liquid extraction method^{23, 29} on the Dionex ASE200
112 system (Dionex, Sunnyvale, CA, USA). Extraction cells (33 mL) loaded with pre-combusted Florisil (12
113 g) and diatomaceous earth (DE, 2 g) were extracted with a mixture of hexane and acetone (1:1, v/v) on an
114 ASE200 at 100 °C and 1500 psi (10 MPa) with preheat equilibration for 6 min, 60% of cell flush volume,
115 and 1 static cycle of 5 min. The tissue was homogenized with the top DE layer, and the DE-tissue mixture

116 was placed back into the extraction cell. Blood samples were loaded directly onto the cellulose filter of
117 the cell. Surrogate standards, d-PCB 30 and d-PCB 65 (80 ng each), were added to every sample before
118 the extraction. The cells were extracted with the same parameters described above. The extracts were
119 concentrated to ~0.5 mL on a TurboVap II (Biotage LLC, NC, USA), transferred to a pre-combusted tube,
120 and treated with 2 mL of concentrated sulfuric acid for lipid removal. The extract was transferred to a
121 new glass tube, evaporated under a gentle stream of nitrogen to ~50 μ L, and transferred to a gas
122 chromatography vial. The internal standards (volume correctors), $^{13}\text{C}_{12}$ -PCB 9 and $^{13}\text{C}_{12}$ -PCB 194 (50 ng
123 each), were spiked to every sample before analysis.

124 ***Gas chromatographic determinations.*** Samples were analyzed using an Agilent 7890A gas
125 chromatograph coupled with an Agilent 5975C Inert Mass Selective Detector (MSD) operated in
126 electronic ionization mode. An SLB-5MS capillary GC column (30 m length, 250 μ m inner diameter,
127 0.25 μ m film thickness; Supelco, Bellefonte, PA, USA) was used in the select ion monitoring (SIM)
128 mode.³⁰⁻³² The temperature program was as follows: 80 $^{\circ}\text{C}$, hold for 1 min, 2 $^{\circ}\text{C}/\text{min}$ to 160 $^{\circ}\text{C}/\text{min}$,
129 1 $^{\circ}\text{C}/\text{min}$ to 170 $^{\circ}\text{C}$, hold for 15 min, 1 $^{\circ}\text{C}/\text{min}$ to 180 $^{\circ}\text{C}$, hold for 15 min, 1 $^{\circ}\text{C}/\text{min}$ to 245 $^{\circ}\text{C}$, t10 $^{\circ}\text{C}/\text{min}$
130 to 300 $^{\circ}\text{C}$, and hold for 15 min. The injector temperature was 280 $^{\circ}\text{C}$, and the operating temperatures
131 were 280 $^{\circ}\text{C}$, 230 $^{\circ}\text{C}$ and 150 $^{\circ}\text{C}$ for transfer line, source, and quadrupole, respectively. The flow rate of
132 carrier gas helium was 1.1 mL/min. By this congener specific method, 162 individual or co-eluting peaks
133 of PCBs can be separated and quantified. Twenty-eight channels were set up in GC-MS SIM mode (see
134 details in Table S1). The MSD was linear over the concentration range encountered in this study (Table
135 S2). For Figures with PCB congener profiles, see Figs. S1-S4. The peak corresponding to PCB 138, PCB
136 158, PCB 163, and PCB 164 is abbreviated as PCB 138 throughout the manuscript.

137 ***Model prediction of the tissue-blood partitioning of PCBs.*** A composition-based model³³ was used
138 for the prediction of the partition coefficients of PCBs between tissues and whole blood. In this model,
139 tissues and blood are assumed to contain five biological components, including albumin, muscle protein,
140 membrane lipid, storage lipid, and water. The volume fractions and lipid content of all biological

141 components, both in tissues and blood, were taken from published experimental values (Table S3).^{23, 33, 34}
 142 The partitioning of PCBs between the biological components was determined with published Abraham
 143 solvation parameters³⁵ and polyparameter linear free energy relationships (PP-LFERs) describing the
 144 correlations between the chemical descriptors and tissue/water partition coefficients.³⁶⁻³⁹ The equation
 145 used for the calculations of tissue-blood partitioning coefficients ($K_{tissue/blood}$) were as follows:³³

$$146 \quad K_{tissue/blood} = \frac{K_{tissue/water}}{K_{blood/water}}$$

$$147 \quad = \frac{K_{ap/w}f_{ap}^{tissue} + K_{mp/w}f_{mp}^{tissue} + K_{sl/w}f_{sl}^{tissue} + K_{ml/w}f_{ml}^{tissue} + f_w^{tissue}}{K_{ap/w}f_{ap}^{blood} + K_{mp/w}f_{mp}^{blood} + K_{sl/w}f_{sl}^{blood} + K_{ml/w}f_{ml}^{blood} + f_w^{tissue}} \quad (1)$$

148 where $K_{tissue/water}$ and $K_{blood/water}$ are the partition coefficients of PCBs between tissue and water and
 149 between blood and water, respectively. $K_{ap/w}$, $K_{mp/w}$, $K_{sl/w}$ and $K_{ml/w}$ are the partition coefficients of
 150 PCBs between albumin protein and water, muscle protein and water, storage lipid and water, and
 151 membrane lipid and water, respectively. f_{ap}^{tissue} , f_{mp}^{tissue} , f_{sl}^{tissue} , f_{ml}^{tissue} and f_w^{tissue} are the volume
 152 fractions of albumin protein, muscle protein, storage lipid, membrane lipid, and water in tissue,
 153 respectively. f_{ap}^{blood} , f_{mp}^{blood} , f_{sl}^{blood} , f_{ml}^{blood} and f_w^{blood} are the volume fractions of albumin protein,
 154 muscle protein, storage lipid, membrane lipid, and water in the blood, respectively.

155 **Data visualization and statistical analysis.** PCBs congener profiles and PCB levels in tissues from
 156 different exposure groups and tissues were analyzed with MetaboAnalyst 4.0.⁴⁰ Similarity coefficients
 157 $\cos \Theta$ were calculated are described previously.²⁴

158 RESULTS AND DISCUSSION

159 **Levels of total PCBs (Σ PCB) in tissues.** In WT mice, the Σ PCB levels followed the rank order
160 adipose > liver ~ brain > blood (Fig. 1). This rank order is consistent with earlier studies reporting an
161 accumulation of PCBs and related organochlorines in fat-rich organs from different mammalian
162 species.¹²⁻¹⁴ In KO mice, the Σ PCB levels in adipose and liver tissue were similar and followed the rank
163 order adipose ~ liver > brain > blood. Similar trends were observed when tissue levels of individual PCB
164 congeners (i.e., PCB 91 and PCB 136) were compared across tissues in WT or KO mice exposed to either
165 Aroclor 1254 (Fig. S5), PCB 91 or PCB 136.^{22, 23} We observed minor genotype and sex-dependent
166 differences in the Σ PCB levels in adipose, blood and brain (Fig. 1). For example, Σ PCB levels were 1.8-
167 times higher in the female than the male liver, a difference that reached statistical significance for WT
168 mice ($3.3 \pm 1.8 \mu\text{g/g}$ vs. $5.9 \pm 1.8 \mu\text{g/g}$ for M and F_w mice, respectively).

169 A drastic enrichment of Σ PCB was observed in the liver of KO compared to WT mice, irrespective of
170 the sex. This difference in the distribution of PCBs was also observed in disposition studies of single PCB
171 congener in KO and WT mice.^{22, 23} The accumulation of PCBs in the liver of KO mice is a consequence
172 of the higher lipid content and the elevated protein levels in the liver of KO compared to WT mice. In
173 turn, the higher lipid content in the liver of KO mice is caused by an impaired hepatic fat metabolism.^{41, 42}
174 In addition to an increased lipid content in the liver, the expression of hepatic proteins that bind PCBs,
175 such as cytochrome P450 enzymes,^{43, 44} is increased in the liver to compensate for the liver-specific
176 deletion of *cpr*.²⁶ For example, dioxin-like PCBs and structurally related compounds are sequestered in
177 the liver because they bind to particular cytochrome P450 isoforms.^{45, 46} Analogously, it is likely that
178 cytochrome P450 enzymes in the liver from KO mice bind PCBs in the absence of metabolic conversion,
179 thus contributing to the hepatic accumulation of PCBs in KO mice.

180 **PCB homolog composition in tissues.** The homolog composition of the PCB residue in the adipose
181 tissue from WT and KO mice, expressed as a mass percentage, was comparable to the homolog
182 composition of Aroclor 1254 (Fig. 1; see Table S4). However, an increase in the percentage of higher

183 chlorinated PCBs was apparent in the adipose tissue from WT mice, irrespective of the sex. The homolog
184 composition of the PCB residues from blood, brain, and liver tissues showed differences compared to the
185 homolog composition of Aroclor 1254. Typically, the percentage of lower chlorinated homologs
186 decreased, whereas the percentage of higher chlorinated homologs increased in tissues compared to
187 Aroclor 1254. More pronounced shifts in the homolog composition were observed for WT compared to
188 KO mice. For example, hexachlorinated PCBs were the major constituents in the brain from F_{WT} mice,
189 whereas pentachlorinated PCBs are the major homolog group in Aroclor 1254 (Table S4). These shifts in
190 the PCB homolog composition are consistent with the more rapid clearance of lower chlorinated PCBs in
191 rodents.^{47, 48}

192 The changes in the homolog mass profiles translated into sex and genotype-dependent differences in
193 PCB homolog levels, adjusted by tissue wet weight, in blood, brain, and liver (Fig. 1; see Table S4).
194 Consistent with the higher Σ PCB levels described above, the levels of all homolog groups in the liver
195 were more elevated in KO compared to WT mice because of the higher fat and protein content of the liver
196 of KO mice. Levels of tetra- and pentachlorinated PCBs were lower in blood from F_{WT} mice compared to
197 all other exposure groups. Moreover, levels of tetra- and pentachlorinated PCBs were lower in the brain
198 of F_{WT} but higher in the brain of F_{KO} mice. For example, levels of pentachlorinated PCBs in the brain of
199 F_{KO} mice were $1,110 \pm 70$ ng/g tissue, which is almost 2-fold higher than the levels in F_{WT} mice (630 ± 70
200 ng/g tissue).

201 ***Distribution of different PCB Classes in tissues.*** Although lower chlorinated PCBs are generally
202 more rapidly metabolized than higher chlorinated PCBs, the metabolism and elimination of PCBs also
203 depend on the chlorine substitution pattern.⁴⁹ Therefore, we compared differences in the mass percentage
204 of PCBs congeners with a 4-, 3,4-, and 3,4,5- substitution pattern and zero or one *ortho* chlorine
205 substituent (Class A); PCB congeners with two or more *ortho* chlorine substituents and a 2,4- or 2,3,4-
206 substitution pattern (Class B); PCB congeners with a 2,4,5-substitution pattern (Class C); and PCB
207 congeners that are considered to be episodic because they are rapidly eliminated following exposure.¹⁶

208 Class D congeners have adjacent, unsubstituted C-atoms and, typically, contain a 2-, 2,3-, 2,5- and 2,3,6-
209 substitution pattern in at least one phenyl ring (Class D).^{50, 51}

210 The mass percentage of PCBs belonging to Class C increased relative to Aroclor 1254 in all tissues
211 from all four exposure groups (Fig. 1; Table S5). This enrichment of Class C congeners is expected
212 because higher chlorinated PCBs with two *para* chlorine, such as PCB 153, are less susceptible to
213 metabolic transformation than PCBs without *para* chlorine substituents. Conversely, the mass percentage
214 of PCBs in Class A decreased in all tissues. The metabolism of (some) Class A congeners is one
215 explanation for the relative decrease in the contribution of this PCB Class to the Σ PCBs. Although PCB
216 congeners with two *para* chlorine substituents are thought to be less susceptible to metabolic conversion,
217 some Class A congeners are readily oxidized by cytochrome P450 enzymes. For example, PCB 77 is
218 readily metabolized in rodents,^{52, 53} and hydroxylated metabolites of PCB 28 have been detected in
219 humans.⁵⁴ Interestingly, the mass percentage of Class D congeners tended to be higher in the adipose
220 tissue and blood, especially in KO mice, and lower in the brain and liver compared to Aroclor 1254.
221 These differences are potentially due to differences in the initial distribution and redistribution of PCBs to
222 the adipose tissue, as well as their (extrahepatic) metabolism.⁵²

223 We also observed differences in the percentage of PCBs when comparing the mass percentages across
224 genotypes and between sexes (Fig. 1; Table S5). The percentage of more persistent PCBs (i.e., Classes A,
225 B, and C) appeared to be higher in WT compared to KO mice, irrespective of the sex. Importantly, the
226 levels of PCBs by Class, expressed as tissue wet weight, revealed similar sex and genotype-dependent
227 differences. These overall trends are consistent with impaired metabolism of PCBs belonging to Class D
228 in WT mice, which ultimately is caused by the lack of CPR activity in the liver. It is noteworthy that this
229 effect was more pronounced in F_{WT} mice, especially in the liver and brain.

230 ***Comparison of PCB profiles in adipose tissue from different exposure groups and Aroclor 1254.***

231 PCB congener profiles in adipose tissues were different from the PCB profile of Aroclor 1254 (cos Θ =
232 0.84 to 0.88; Table S6). In contrast, PCB profiles in adipose tissue were quite similar across all four

233 exposure groups ($\cos \Theta = 0.97$ to 1.0 ; Table S7). Further analysis of individual PCB congeners revealed
234 minor genotype and, for some congeners, sex-dependent differences in the adipose tissue (Fig. 2a).
235 Persistent PCB congeners, for example PCB 118 (Class A) and PCB 180 (Class C), contained a relatively
236 higher percentage in adipose tissue from WT mice. In contrast, PCB congeners belonging to Class D,
237 such as PCB 70, PCB 95, and PCB 136, showed the opposite trend, with lower percentages of these PCB
238 congeners being present in the adipose tissue from WT compared to KO mice. Moreover, the percentage
239 of many Class D congeners were lower in F_{WT} mice compared to the other exposure groups. Importantly,
240 the differences in the PCB congener profiles typically did not result in differences in the PCB levels in the
241 adipose tissue (Fig. S6a). This finding is not surprising because the high PCB content masks small
242 differences in PCB levels in the adipose tissue.

243 ***Comparison of PCB profiles in whole blood from different exposure groups and Aroclor 1254.*** PCB
244 congener profiles in blood were different from the PCB profile of Aroclor 1254 ($\cos \Theta = 0.72$ to 0.74 ;
245 Table S6). The percentage of major PCB congeners present in Aroclor 1254 (e.g., PCB 70) decreased in
246 blood from all four exposure groups (Fig. 2b). Irrespective of the sex, PCB 138 (analyzed as a peak of
247 four co-eluting PCB congeners) was the major PCB congener in WT mice. PCB 101 was the major PCB
248 congener in blood from KO mice. The percentages of other PCB congeners, for example PCB 95 and
249 PCB 180, increased in blood from all exposure groups compared to Aroclor 1254 (Fig. 2b). PCB 52, a
250 PCB congener that is structurally similar to PCB 95, was the third most abundant PCB congener detected
251 in blood (8.1 to 9.0 % in blood vs. 1.7 % in Aroclor 1254). The same PCB congeners are among the most
252 abundant PCB congeners detected in serum samples from the MARBLES cohort, a group of pregnant
253 women at risk of having a child with a neurodevelopmental disorder.⁵⁵ PCB 52, PCB 95, and PCB 101
254 are among the twenty most frequently detected PCB congeners in air and in humans.⁵⁶

255 The congener profiles revealed minor genotype-dependent differences in the blood ($\cos \Theta = 0.98$ to
256 0.99 , Table S7). F_{WT} mice were an exception and displayed a PCB congener profile that was different
257 from the profiles observed in the blood from the other exposure groups ($\cos \Theta = 0.92$ to 0.97). The

258 percentage of some congeners (e.g., PCB 70) was higher in KO compared to WT mice (Fig. 2b). Different
259 congeners (e.g., PCB 99 and PCB 180) had a lower percentage in KO compared to WT mice. In the blood
260 from F_{WT} mice, PCB congeners belonging to Class D were present at a lower mass percentage, and more
261 persistent PCB congeners from Classes A, B, and C were present at a higher mass percentage compared
262 to M_{WT}, F_{KO}, and M_{KO}. Similar trends between KO and WT mice were observed for these congeners when
263 comparing PCB levels adjusted for wet weight (Fig. S6b). For example, PCB 95 levels, expressed on a
264 wet weight basis, were lower in the blood from F_{WT} mice (8±1 ng/g wet weight) compared to the other
265 exposure groups (13 to 14 ng/g wet weight, depending on the exposure group).

266 ***Comparison of PCB profiles in the brain from different exposure groups and Aroclor 1254.*** PCB
267 residues in the brain from all exposure groups were distinctively different from the Aroclor 1254 profile
268 (Fig. 2c), with similarity coefficients ranging from 0.80 to 0.86 (Table S6). PCB 138 (analyzed as a peak
269 of four co-eluting PCB congeners) and PCBs 132/153 were the two dominant PCB congeners in the brain
270 from both WT and KO mice. PCB 118, the dominant PCB congener in Aroclor 1254 (12.6 %),
271 contributed a similar percentage to the ΣPCBs in all exposure groups (9.8 to 12.3 %). These PCBs were
272 also prevalent PCB congeners detected in the brain from postnatal day 31 rats exposed to Aroclor 1254
273 throughout development via the maternal.⁵⁷ PCB 138, PCB 153 and PCB 118 were also prevalent PCB
274 congener in postmortem human brain samples.^{58,59} Unlike the present study, these studies analyzed a
275 small set of PCB congeners and, thus, provide limited insights into the congener profiles present in the
276 rodent or human brain.

277 The PCB congener profiles in the brain showed genotype and sex-dependent differences (Fig. 2c),
278 with similarity coefficients ranging from 0.96 to 0.99 (Table S7). Many congeners belonging to Class D
279 (e.g., PCB 136) were lower in F_{WT} mice compared to the other exposure groups, especially F_{KO} mice. The
280 differences observed in the congener profiles F_{WT} compared to F_{KO} mice translated into differences in the
281 levels of Class D congeners in the brain (Fig. S6c), an observation that is toxicologically relevant. For
282 example, PCB 95 and PCB 136 are potent sensitizers of the ryanodine receptors,⁶⁰ cellular targets

283 implicated in PCB-induced developmental neurotoxicity.^{30, 61, 62} PCB mixtures (i.e., Aroclor 1254) and
284 PCB 95 display a non-monotonic dose-response relationship in rodent studies of PCB developmental
285 neurotoxicity.^{57, 63} Thus, depending on the experimental design and the dose, relatively small differences
286 in the levels of potent, neurotoxic PCB congeners in the developing brain may significantly affect
287 neurotoxic outcomes. In the present study, levels of PCB 95 and PCB 136 were 1.4- and 3.0-fold higher
288 in the brain from F_{KO} compared to F_{WT} mice, respectively. Further studies are needed to assess if similar
289 differences in the levels of these neurotoxic PCB congeners are present in the fetal and neonatal brain of
290 KO compared to WT mice exposed to PCBs.

291 ***Comparison of PCB profiles in the liver from different exposure groups and Aroclor 1254.*** PCB
292 profiles in the liver were clearly different from the profile observed for Aroclor 1254 (Fig. 2d), with
293 similarity coefficients ranging from 0.77 to 0.88 (Table S6). PCB congener profiles in the liver of M_{WT},
294 M_{KO}, and F_{KO} mice showed only small differences, with similarity coefficients of 0.97 to 1.0. (Table S7).
295 As with blood and brain tissue, more pronounced differences were observed for F_{WT} mice compared to
296 the other exposure groups (similarity coefficient 0.92 to 0.93; Table S7). Levels of individual PCB
297 congeners were always much higher in KO compared to WT mice, irrespective of the sex, because of the
298 higher fat and protein content of the liver of KO mice (Fig. S6d).^{26, 41, 42}

299 Female mice had higher levels of specific PCB congeners in the liver than male mice of the same
300 genotype; however, this difference typically did not reach statistical significance (t-test, $p > 0.05$). We
301 observed a similar trend when comparing PCB levels on a Σ PCB and PCB homolog basis (Fig. 1). Sex
302 differences in PCB levels of WT mice, especially in the liver, would be consistent with the higher
303 expression of Cyp2b10, a cytochrome P450 isoform implicated in the metabolism on Class D PCB
304 congeners,⁶⁴ and other hepatic and extrahepatic cytochrome P450 enzymes in the female compared to the
305 male mouse liver.⁶⁵ Indeed, PCB 136 is more rapidly oxidized in precision-cut tissue slices from male
306 compared to female rats.⁶⁶ However, no sex-dependent differences in PCB levels have been reported in
307 earlier disposition studies in rodents after developmental PCB exposure.^{57, 67-69} These observations suggest

308 that sex-dependent differences in the hepatic metabolism of PCBs have only a small effect on PCB tissue
309 levels and, possibly, toxic outcomes, at least in rodent models.

310 ***Differences in PCB profiles in tissues from the same exposure group.*** Laboratory and biomonitoring
311 studies generally assume that the profiles and levels of PCB in the blood are a reasonable approximation
312 of tissue profiles and levels. For example, the distribution of PCBs in juvenile rats shows that serum
313 levels are predictive of liver levels;¹⁵ however, studies that investigate the congener-specific distribution
314 of PCBs across tissues are limited, especially for lower chlorinated PCBs. In the present study, PCB
315 profiles displayed modest differences between tissues within each exposure group, as indicated by tissue-
316 to-tissue similarity coefficients ranging from 0.85 to 0.98 (Table S8; Fig. S7). Several other animal
317 studies also reported modest inter-tissue differences in the PCB profiles after oral or inhalation exposure
318 ($\cos \Theta \geq 0.80$).^{6, 32, 70}

319 Sparse partial least squares-discriminant analysis (sPLS-DA) was used to investigate differences in the
320 PCB profiles across tissues within the same exposure group (Fig 3; Figs. S8-S10). sPLS-DA comparing
321 the PCB congener profiles from F_{WT} mice showed clear groupings according to tissue, with three
322 principal components (PCs) accounting for 84.6% of the data variance (Fig. 3). PC1 separated adipose
323 tissue from the brain and liver. Based on their loadings, PCB congeners belonging to Class D (i.e., PCB
324 52 and PCB 70) were higher in adipose tissue, but lower in brain and liver. PCBs belonging to Class B
325 (i.e., PCB 138) and Class C (i.e., PCB 146 and PCB 183) made a lower contribution to the PCB profile in
326 adipose tissue, but a higher contribution in the brain and liver. PC2 separated blood from adipose tissue,
327 with some Class D congener (i.e., PCB 139/149 and PCB 151) being higher in blood, but lower in
328 adipose tissue and liver. PC3 separated the liver from other tissues because of lower relative levels of
329 Class D congeners (i.e., PCBs 134/143 and PCB 136). Overall, differences in the PCB congener profiles
330 across tissues from W_{WT} were due to differences in the percentage of metabolically more labile PCB
331 congeners (Class D) compared to congeners resistant to metabolites (Class A through C). Similar
332 differences in the PCB congener profiles across tissues were observed for the other exposure groups

333 despite the impaired hepatic metabolism in KO mice (Figs. S8-S10). In general, these comparisons
334 support the assumption that PCB profiles in the blood are a reasonable approximation of PCB tissue
335 profiles in mice and other mammals.

336 ***Tissue-to-blood distribution of PCBs within each exposure group.*** The distribution of individual
337 congener from the blood into tissues has toxicological relevance. Tissue : blood ratios followed the rank
338 order adipose : blood (median: 201; range: 12-841) >> liver : blood (median: 22; range: 7-213) > brain :
339 blood (median: 11; range: 3-34) in WT mice. This rank order is consistent with earlier studies in mice
340 and other mammalian models.¹¹ The differences between liver : blood vs. brain : blood partition
341 coefficients were more pronounced in KO mice because of the higher lipid content in the liver, with
342 adipose : blood (median: 71; range: 40-470) ~ liver : blood (median: 91; range 47-481) >> brain : blood
343 (median: 5; range 3-28). With the exception of the liver : blood partition coefficients in KO mice, the
344 partition coefficients in this study are within the range of partition coefficients observed in animal studies
345 and in humans.^{11,71} For example, adipose to plasma partition coefficients of 24 PCB congeners in
346 occupationally exposed individuals ranged from 50 to 370.⁷¹

347 The partitioning of PCBs between tissues and blood changed with increasing degree of chlorination.
348 For example, tetra- to hexachlorinated PCBs appeared to have a much higher affinity for adipose tissue
349 than higher chlorinated homologs in F_{WT} mice at the time point investigated (Fig. 4). The opposite was
350 true for the brain, where the partitioning into the brain appeared to increase with an increase in
351 chlorination. The partitioning of PCBs from the blood into the liver from F_{WT} mice seemed to be
352 comparable across homolog groups. Similar trends were observed for M_{WT}, M_{KO}, and F_{KO} mice (Figs.
353 S11-S13). The decrease in the adipose : blood partitioning by the homolog group is unexpected based on
354 a structure-based model of the tissue-to-blood partitioning of PCBs.⁷² Besides, the partitioning of
355 individual congeners from the blood into tissues was congener-specific and displayed considerable
356 variability (Figs. 4a-c). Thus, congener specific differences in the blood-to-tissue partitioning exist at
357 specific time points that may influence toxic outcomes following PCB exposure. These differences are

358 not captured when, as discussed above, only PCB profiles are compared between tissues. Especially
359 systematic studies of tissue : blood ratios in human postmortem samples remain limited,⁷³⁻⁷⁵ and further
360 congener-specific studies are needed, especially for lower chlorinated PCB congeners that, unlike
361 persistent legacy PCBs, are still inadvertently produced and represent a current public health concern.⁵⁶

362 ***Comparison of the experimental and theoretical tissue-to-blood distribution of PCBs.*** A number of
363 models have been developed to predict the partition coefficients in tissues in the absence of experimental
364 data, including tissue composition-based models.^{33, 34} These models use readily available information,
365 including the quantities of the biological components (e.g., lipids, protein, and water) in tissues and the
366 partition coefficients of PCBs (e.g., lipid/water partitioning coefficient), to estimate the distribution of
367 PCBs *in vivo*. For example, a PP-LFER-composition-based model was adopted to determine the liver :
368 blood partitioning coefficients mono- to hexachlorinated PCBs and the adipose : plasma partition
369 coefficients of di- to octa-chlorinated PCBs in rats.³³ This model has several advantages: It can be used to
370 predict the partitioning of PCBs between the biological components of all PCB congeners can be
371 described with published Abraham solvation parameters³⁵ and PP-LFERs describing the correlations
372 between the chemical descriptors and tissue/water partition coefficients.³⁶⁻³⁹ Moreover, this model should
373 be able to estimate the tissue : blood partitioning of PCBs in mouse models with a fatty liver.

374 The theoretical tissue : blood ratios, determined with this published model,³³ are shown for all 209
375 PCB congeners in Fig. 4d. The model did not predict the congener-specific variability of the partition
376 coefficients. Moreover, the model predicted an increase, not a decrease in the adipose : blood ratios with
377 increasing degree of chlorination. These differences between the calculated and experimental value are
378 not entirely surprising because the model does not take structural features into account that, for example,
379 influence the rate of metabolism of individual PCB congeners. Moreover, individual PCBs probably had
380 not reached steady-state levels in our study. The model also overestimated the partitioning of PCBs into
381 the brain. Similarly, earlier studies noted that the levels of PCBs in the brain are lower than expected

382 based on the lipid content of the brain, a fact that can be explained with the unique lipid composition of
383 the human brain.^{58, 76}

384 Despite these differences, the predicted and experimental partition coefficients were in reasonable
385 agreement with each other (i.e., deviations were within one order of magnitude, Fig. 4e) and matched the
386 calculated adipose : blood partition coefficients in rats.³³ The model correctly predicted the more
387 pronounced partitioning of PCBs into the liver of KO mice. While not perfect, composition-based models
388 are, therefore, an effective tool to approximate tissue levels based on blood PCB levels, which are
389 experimentally more accessible, especially in humans. However, more detailed, PCB congener-specific
390 studies of the PCB levels in human tissues and blood from the same donors are needed to establish
391 whether or not the model used in our research also allows a rough estimate of PCB tissue levels based on
392 experimentally determined blood levels. Additional work is also necessary to better predict the
393 partitioning of PCBs into brain tissues.

394 CONFLICT OF INTEREST STATEMENT

395 The authors declare no competing financial interest.

396 FUNDING SOURCES

397 This work was supported by grants ES027169, ES013661, and ES005605 from the National
398 Institute of Environmental Health Sciences, National Institutes of Health. The content is solely
399 the responsibility of the authors and does not necessarily represent the official views of the
400 National Institute of Environmental Health Sciences or the National Institutes of Health.

401 ACKNOWLEDGMENTS

402 The authors thank Dr. Xinxin Ding (University of Arizona, Tucson, Arizona) for providing the mouse
403 model.

404 SUPPORTING INFORMATION

405 Details regarding GC-MS parameters and the detector response for individual PCB congeners, the
406 biological composition of mouse tissues, PCB composition by homolog group and class, similarity
407 coefficients, PCB congener profiles in tissues, levels of PCB 91 and PCB 136 in tissues from KO and WT
408 mice, comparison of the PCB levels and congener profiles in different tissues, sPLS-DA comparing PCB
409 congener profiles in tissues from M_{WT} , M_{KO} and F_{KO} mice, tissue : blood ratios of different PCB homolog
410 groups in M_{WT} , M_{KO} and F_{KO} mice; and predicted tissue : blood ratios. This material is available free of
411 charge via the Internet at <http://pubs.acs.org>.

412 REFERENCES

- 413 1. ATSDR, Toxicological Profile for Polychlorinated Biphenyls (PCBs).
414 <https://www.atsdr.cdc.gov/toxprofiles/tp.asp?id=142&tid=26> (accessed 3/21/2020).
- 415 2. Ampleman, M. D.; Martinez, A.; DeWall, J.; Rawn, D. F.; Hornbuckle, K. C.; Thorne, P.
416 S., Inhalation and dietary exposure to PCBs in urban and rural cohorts via congener-
417 specific measurements. *Environ. Sci. Technol.* **2015**, *49*, 1156-1164.
- 418 3. Chen, X.; Lin, Y.; Dang, K.; Puschner, B., Quantification of polychlorinated biphenyls
419 and polybrominated diphenyl ethers in commercial cows' milk from California by gas
420 chromatography-triple quadruple mass spectrometry. *PLoS One* **2017**, *12*, e0170129.
- 421 4. Schechter, A.; Colacino, J.; Haffner, D.; Patel, K.; Opel, M.; Papke, O.; Birnbaum, L.,
422 Perfluorinated compounds, polychlorinated biphenyls, and organochlorine pesticide
423 contamination in composite food samples from Dallas, Texas, USA. *Environ. Health*
424 *Perspect.* **2010**, *118*, 796-802.
- 425 5. Hu, X.; Adamcakova-Dodd, A.; Lehmler, H.-J.; Hu, D.; Kania-Korwel, I.; Hornbuckle,
426 K. C.; Thorne, P. S., Time course of congener uptake and elimination in rats after short-
427 term inhalation exposure to an airborne polychlorinated biphenyl (PCB) mixture.
428 *Environ. Sci. Technol.* **2010**, *44*, 6893-6900.
- 429 6. Hu, X.; Adamcakova-Dodd, A.; Lehmler, H. J.; Hu, D.; Hornbuckle, K.; Thorne, P. S.,
430 Subchronic inhalation exposure study of an airborne polychlorinated biphenyl mixture
431 resembling the Chicago ambient air congener profile. *Environ. Sci. Technol.* **2012**, *46*,
432 9653-9662.

- 433 7. Hu, X.; Lehmler, H. J.; Adamcakova-Dodd, A.; Thorne, P. S., Elimination of inhaled
434 3,3'-dichlorobiphenyl and the formation of the 4-hydroxylated metabolite. *Environ. Sci.*
435 *Technol.* **2013**, *47*, 4743-4751.
- 436 8. Kania-Korwel, I.; Barnhart, C. D.; Stamou, M.; Truong, K. M.; El-Komy, M. H.; Lein, P.
437 J.; Veng-Pedersen, P.; Lehmler, H.-J., 2,2',3,5',6-Pentachlorobiphenyl (PCB 95) and its
438 hydroxylated metabolites are enantiomerically enriched in female mice. *Environ. Sci.*
439 *Technol.* **2012**, *46*, 11393-11401.
- 440 9. Kania-Korwel, I.; El-Komy, M. H. M. E.; Veng-Pedersen, P.; Lehmler, H.-J., Clearance
441 of polychlorinated biphenyl atropisomers is enantioselective in female C57Bl/6 mice.
442 *Environ. Sci. Technol.* **2010**, *44*, 2828-2835.
- 443 10. Birnbaum, L. S., Distribution and excretion of 2,3,6,2',3',6'- and 2,4,5,2',4',5'-
444 hexachlorobiphenyl in senescent rats. *Toxicol. Appl. Pharmacol.* **1983**, *70*, 262-272.
- 445 11. Lutz, R. J.; Dedrick, R. L.; Tuey, D.; Sipes, I. G.; Anderson, M. W.; Matthews, H. B.,
446 Comparison of the pharmacokinetics of several polychlorinated biphenyls in mouse, rat,
447 dog, and monkey by means of a physiological pharmacokinetic model. *Drug Metab.*
448 *Dispos.* **1984**, *12*, 527-535.
- 449 12. Kania-Korwel, I.; Hornbuckle, K. C.; Peck, A.; Ludewig, G.; Robertson, L. W.;
450 Sulkowski, W. W.; Espandiari, P.; Gairola, C. G.; Lehmler, H.-J., Congener specific
451 tissue distribution of Aroclor 1254 and a highly chlorinated environmental PCB mixture
452 in rats. *Environ. Sci. Technol.* **2005**, *39*, 3513-3520.
- 453 13. Milanowski, B.; Lulek, J.; Lehmler, H.-J.; Kania-Korwel, I., Assessment of the
454 disposition of chiral polychlorinated biphenyls in female mdr 1a/b knockout versus wild-
455 type mice using multivariate analyses. *Environ. Int.* **2010**, *36*, 884-892.

- 456 14. Weisbrod, A. V.; Shea, D.; Moore, M. J.; John, J. J., Bioaccumulation patterns of
457 polychlorinated biphenyls and chlorinated pesticides in Northwest Atlantic pilot whales.
458 *Environ. Toxicol. Chem.* **2000**, *19*, 667-677.
- 459 15. Soontornchat, S.; Li, M. H.; Cooke, P. S.; Hansen, L. G., Toxicokinetic and
460 toxicodynamic influences on endocrine disruption by polychlorinated biphenyls. *Environ.*
461 *Health Perspect.* **1994**, *102*, 568-571.
- 462 16. Imsilp, K.; Hansen, L., PCB profiles in mouse skin biopsies and fat from an
463 environmental mixture. *Environ. Toxicol. Pharmacol.* **2005**, *19*, 71-84.
- 464 17. Hansen, L. G.; Welborn, M. E., Distribution, dilution, and elimination of polychlorinated
465 biphenyl analogs in growing swine. *J. Pharm. Sci.* **1977**, *66*, 497-501.
- 466 18. Wyss, P. A.; Muehlebach, S.; Bickel, M. H., Pharmacokinetics of 2,2',4,4',5,5'-
467 hexachlorobiphenyl (6-CB) in rats with decreasing adipose tissue mass. I. Effects of
468 restricting food intake two weeks after administration of 6-CB. *Drug Metab. Dispos.*
469 **1982**, *10*, 657-661.
- 470 19. Spindler-Vomachka, M.; Vodcnik, M. J., Distribution of 2,4,5,2',4',5'-
471 hexachlorobiphenyl among lipoproteins during pregnancy and lactation in the rat. *J.*
472 *Pharmacol. Exp. Ther.* **1984**, *230*, 263-268.
- 473 20. Chu, I.; Villeneuve, D. C.; Yagminas, A.; Lecavalier, P.; Poon, R.; Feeley, M.; Kennedy,
474 S. W.; Seegal, R. F.; Hakansson, H.; Ahlborg, U. G.; Valli, V. E., Subchronic toxicity of
475 3,3',4,4',5-pentachlorobiphenyl in the rat. 1. Clinical, biochemical, hematological, and
476 histopathological changes. *Fundam. Appl. Toxicol.* **1994**, *22*, 457-468.
- 477 21. Van Birgelen, A. P. J. M.; Van der Kolk, J.; Fase, K. M.; Bol, I.; Poiger, H.; Brouwer, A.;
478 Van den Berg, M., Toxic potency of 3,3',4,4',5-pentachlorobiphenyl relative to and in

- 479 combination with 2,3,7,8-tetrachlorodibenzo-*p*-dioxin in a subchronic feeding study in
480 the rat. *Toxicol. Appl. Pharmacol.* **1994**, *127*, 209-221.
- 481 22. Wu, X.; Zhai, G.; Schnoor, J. L.; Lehmler, H.-J., Atropselective disposition of 2,2',3,4',6-
482 pentachlorobiphenyl (PCB 91) and identification of its metabolites in mice with liver-
483 specific deletion of cytochrome P450 reductase. *Chem. Res. Toxicol.* **2020**. DOI:
484 10.1021/acs.chemrestox.9b00255.
- 485 23. Wu, X.; Barnhart, C.; Lein, P. J.; Lehmler, H. J., Hepatic metabolism affects the
486 atropselective disposition of 2,2',3,3',6,6'-hexachlorobiphenyl (PCB 136) in mice.
487 *Environ. Sci. Technol.* **2015**, *49*, 616-625.
- 488 24. Zhao, H.; Adamcakova-Dodd, A.; Hu, D.; Hornbuckle, K. C.; Just, C. L.; Robertson, L.
489 W.; Thorne, P. S.; Lehmler, H.-J., Development of a synthetic PCB mixture resembling
490 the average polychlorinated biphenyl profile in Chicago air. *Environ. Int.* **2010**, *36*, 819-
491 827.
- 492 25. US EPA. Polychlorinated Biphenyls (PCBs). Table of Polychlorinated Biphenyl (PCB)
493 Congeners. <https://www.epa.gov/pcbs/table-polychlorinated-biphenyl-pcb-congeners>
494 (accessed 3/21/2020).
- 495 26. Gu, J.; Weng, Y.; Zhang, Q. Y.; Cui, H.; Behr, M.; Wu, L.; Yang, W.; Zhang, L.; Ding,
496 X., Liver-specific deletion of the NADPH-cytochrome P450 reductase gene: impact on
497 plasma cholesterol homeostasis and the function and regulation of microsomal
498 cytochrome P450 and heme oxygenase. *J. Biol. Chem.* **2003**, *278*, 25895-25901.
- 499 27. Wu, L.; Gu, J.; Weng, Y.; Kluetzman, K.; Swiatek, P.; Behr, M.; Zhang, Q. Y.; Zhuo, X.;
500 Xie, Q.; Ding, X., Conditional knockout of the mouse NADPH-cytochrome P450
501 reductase gene. *Genesis* **2003**, *36*, 177-181.

- 502 28. Li, X.; Wu, X.; Kelly, K. M.; Veng-Pedersen, P.; Lehmler, H.-J., Toxicokinetics of chiral
503 PCB 136 and its hydroxylated metabolites in mice with a liver-specific deletion of
504 cytochrome P450 reductase. *Chem. Res. Toxicol.* **2019**, *32*, 727-736.
- 505 29. Kania-Korwel, I.; Shaikh, N. S.; Hornbuckle, K. C.; Robertson, L. W.; Lehmler, H.-J.,
506 Enantioselective disposition of PCB 136 (2,2',3,3',6,6'-hexachlorobiphenyl) in C57BL/6
507 mice after oral and intraperitoneal administration. *Chirality* **2007**, *19*, 56-66.
- 508 30. Holland, E. B.; Feng, W.; Zheng, J.; Dong, Y.; Li, X.; Lehmler, H.-J.; Pessah, I. N., An
509 extended structure-activity relationship of non-dioxin-like PCBs evaluates and supports
510 modeling predictions and identifies picomolar potency of PCB 202 towards ryanodine
511 receptors. *Toxicol. Sci.* **2016**, *155*, 170-181.
- 512 31. Li, X.; Holland, E. B.; Feng, W.; Zheng, J.; Dong, Y.; Pessah, I. N.; Duffel, M. W.;
513 Robertson, L. W.; Lehmler, H.-J., Authentication of synthetic environmental
514 contaminants and their (bio)transformation products in toxicology: polychlorinated
515 biphenyls as an example. *Environ. Sci. Poll. Res.* **2018**, *25*, 16508-16521.
- 516 32. Hu, X.; Adamcakova-Dodd, A.; Lehmler, H. J.; Gibson-Corley, K.; Thorne, P. S.,
517 Toxicity evaluation of exposure to an atmospheric mixture of polychlorinated biphenyls
518 by nose-only and whole-body inhalation regimens. *Environ. Sci. Technol.* **2015**, *49*,
519 11875-11883.
- 520 33. Endo, S.; Brown, T. N.; Goss, K. U., General model for estimating partition coefficients
521 to organisms and their tissues using the biological compositions and polyparameter linear
522 free energy relationships. *Environ. Sci. Technol.* **2013**, *47*, 6630-6639.
- 523 34. Schmitt, W., General approach for the calculation of tissue to plasma partition
524 coefficients. *Toxicol. In Vitro* **2008**, *22*, 457-467.

- 525 35. van Noort, P. C.; Haftka, J. J.; Parsons, J. R., Updated Abraham solvation parameters for
526 polychlorinated biphenyls. *Environ. Sci. Technol.* **2010**, *44*, 7037-7042.
- 527 36. Endo, S.; Goss, K. U., Serum albumin binding of structurally diverse neutral organic
528 compounds: data and models. *Chem. Res. Toxicol.* **2011**, *24*, 2293-2301.
- 529 37. Endo, S.; Bauerfeind, J.; Goss, K. U., Partitioning of neutral organic compounds to
530 structural proteins. *Environ. Sci. Technol.* **2012**, *46*, 12697-12703.
- 531 38. Geisler, A.; Endo, S.; Goss, K. U., Partitioning of organic chemicals to storage lipids:
532 elucidating the dependence on fatty acid composition and temperature. *Environ. Sci.*
533 *Technol.* **2012**, *46*, 9519-9524.
- 534 39. Endo, S.; Escher, B. I.; Goss, K. U., Capacities of membrane lipids to accumulate neutral
535 organic chemicals. *Environ. Sci. Technol.* **2011**, *45*, 5912-5921.
- 536 40. Chong, J.; Soufan, O.; Li, C.; Caraus, I.; Li, S.; Bourque, G.; Wishart, D. S.; Xia, J.,
537 MetaboAnalyst 4.0: towards more transparent and integrative metabolomics analysis.
538 *Nucleic Acids Res.* **2018**, *46*, W486-W494.
- 539 41. Gu, J.; Cui, H.; Behr, M.; Zhang, L.; Zhang, Q.-Y.; Yang, W.; Hinson, J. A.; Ding, X., *In*
540 *vivo* mechanisms of tissue-selective drug toxicity: effects of liver-specific knockout of
541 the NADPH-cytochrome P450 reductase gene on acetaminophen toxicity in kidney, lung,
542 and nasal mucosa. *Mol. Pharmacol.* **2005**, *67*, 623-630.
- 543 42. Weng, Y.; DiRusso, C. C.; Reilly, A. A.; Black, P. N.; Ding, X., Hepatic gene expression
544 changes in mouse models with liver-specific deletion or global suppression of the
545 NADPH-cytochrome P450 reductase gene. Mechanistic implications for the regulation of
546 microsomal cytochrome P450 and the fatty liver phenotype. *J. Biol. Chem.* **2005**, *280*,
547 31686-31698.

- 548 43. Kania-Korwel, I.; Hrycay, E. G.; Bandiera, S. M.; Lehmler, H.-J., 2,2',3,3',6,6'-
549 Hexachlorobiphenyl (PCB 136) atropisomers interact enantioselectively with hepatic
550 microsomal cytochrome P450 enzymes. *Chem. Res. Toxicol.* **2008**, *21*, 1295-1303.
- 551 44. Kennedy, M. W.; Carpentier, N. K.; Dymerski, P. P.; Kaminsky, L. S., Metabolism of
552 dichlorobiphenyls by hepatic microsomal cytochrome P-450. *Biochem. Pharmacol.* **1981**,
553 *30*, 577-588.
- 554 45. Diliberto, J. J.; Burgin, D. E.; Birnbaum, L. S., Effects of CYP1A2 on disposition of
555 2,3,7,8-tetrachlorodibenzo-*p*-dioxin, 2,3,4,7,8-pentachlorodibenzofuran, and 2,2',4,4',5,5'-
556 hexachlorobiphenyl in CYP1A2 knockout and parental (C57BL/6N and 129/Sv) strains
557 of mice. *Toxicol. Appl. Pharmacol.* **1999**, *159*, 52-64.
- 558 46. Chen, J. J.; Chen, G. S.; Bunce, N. J., Inhibition of CYP 1A2-dependent MROD activity
559 in rat liver microsomes: An explanation of the hepatic sequestration of a limited subset of
560 halogenated aromatic hydrocarbons. *Environ. Toxicol.* **2003**, *18*, 115-119.
- 561 47. Matthews, H. B.; Anderson, M. W., Effect of chlorination on the distribution and
562 excretion of polychlorinated biphenyls. *Drug Metab. Dispos.* **1975**, *3*, 371-380.
- 563 48. Lucier, G. W.; McDaniel, O. S.; Schiller, C. M.; Matthews, H. B., Structural
564 requirements for the accumulation of chlorinated biphenyl metabolites in the fetal rat
565 intestine. *Drug Metab. Dispos.* **1978**, *6*, 584-590.
- 566 49. Birnbaum, L. S., The role of structure in the disposition of halogenated aromatic
567 xenobiotics. *Environ. Health Perspect.* **1985**, *61*, 11-20.
- 568 50. Haraguchi, K.; Koga, N.; Kato, Y., Comparative metabolism of polychlorinated
569 biphenyls and tissue distribution of persistent metabolites in rats, hamsters, and guinea
570 pigs. *Drug Metab. Dispos.* **2005**, *33*, 373-380.

- 571 51. Matthews, H. B.; Tuey, D. B., The effect of chlorine position on the distribution and
572 excretion of four hexachlorobiphenyl isomers. *Toxicol. Appl. Pharmacol.* **1980**, *53*, 377-
573 388.
- 574 52. Saghir, S. A.; Koritz, G. D.; Hansen, L. G., Short Term Distribution, Metabolism, and
575 Excretion of 2,2',5-Tri-, 2,2',4,4'-Tetra-, and 3,3',4,4'-Tetrachlorobiphenyls in Prepubertal
576 Rats. *Arch. Environ. Contam. Toxicol.* **1999**, *36*, 213-220.
- 577 53. Darnerud, P. O.; Sinjari, T.; Jonsson, C. J., Foetal uptake of coplanar polychlorinated
578 biphenyl (PCB) congeners in mice. *Pharmacol. Toxicol.* **1996**, *78*, 187-192.
- 579 54. Quinete, N.; Esser, A.; Kraus, T.; Schettgen, T., PCB 28 metabolites elimination kinetics
580 in human plasma on a real case scenario: Study of hydroxylated polychlorinated biphenyl
581 (OH-PCB) metabolites of PCB 28 in a highly exposed German Cohort. *Toxicol. Lett.*
582 **2017**, *276*, 100-107.
- 583 55. Sethi, S.; Morgan, R. K.; Peng, W.; Lin, Y. P.; Li, X. S.; Luna, C.; Koch, M.; Bansal, R.;
584 Duffel, M. W.; Puschner, B.; Zoeller, R. T.; Lehmler, H. J.; Pessah, I. N.; Lein, P. J.,
585 Comparative analyses of the 12 most abundant PCB congeners detected in human
586 maternal serum for activity at the thyroid hormone receptor and ryanodine receptor.
587 *Environ. Sci. Technol.* **2019**, *53*, 3948-3958.
- 588 56. Grimm, F. A.; Hu, D.; Kania-Korwel, I.; Lehmler, H. J.; Ludewig, G.; Hornbuckle, K. C.;
589 Duffel, M. W.; Bergman, A.; Robertson, L. W., Metabolism and metabolites of
590 polychlorinated biphenyls. *Crit. Rev. Toxicol.* **2015**, *45*, 245-272.
- 591 57. Yang, D.; Kim, K. H.; Phimister, A.; Bachstetter, A. D.; Ward, T. R.; Stackman, R. W.;
592 Mervis, R. F.; Wisniewski, A. B.; Klein, S. L.; Kodavanti, P. R.; Anderson, K. A.;
593 Wayman, G.; Pessah, I. N.; Lein, P. J., Developmental exposure to polychlorinated

594 biphenyls interferes with experience-dependent dendritic plasticity and ryanodine
595 receptor expression in weanling rats. *Environ. Health Perspect.* **2009**, *117*, 426-435.

596 58. Dewailly, E.; Mulvad, G.; Pedersen, H. S.; Ayotte, P.; Demers, A.; Weber, J. P.; Hansen,
597 J. C., Concentration of organochlorines in human brain, liver, and adipose tissue autopsy
598 samples from Greenland. *Environ. Health Perspect.* **1999**, *107*, 823-828.

599 59. Mitchell, M. M.; Woods, R.; Chi, L. H.; Schmidt, R. J.; Pessah, I. N.; Kostyniak, P. J.;
600 LaSalle, J. M., Levels of select PCB and PBDE congeners in human postmortem brain
601 reveal possible environmental involvement in 15q11-q13 duplication autism spectrum
602 disorder. *Environ. Mol. Mutagen.* **2012**, *53*, 589-598.

603 60. Pessah, I. N.; Hansen, L. G.; Albertson, T. E.; Garner, C. E.; Ta, T. A.; Do, Z.; Kim, K.
604 H.; Wong, P. W., Structure-activity relationship for noncoplanar polychlorinated
605 biphenyl congeners toward the ryanodine receptor-Ca²⁺ channel complex type 1 (RyR1).
606 *Chem. Res. Toxicol.* **2006**, *19*, 92-101.

607 61. Pessah, I. N.; Cherednichenko, G.; Lein, P. J., Minding the calcium store: Ryanodine
608 receptor activation as a convergent mechanism of PCB toxicity. *Pharmacol. Ther.* **2010**,
609 *125*, 260-285.

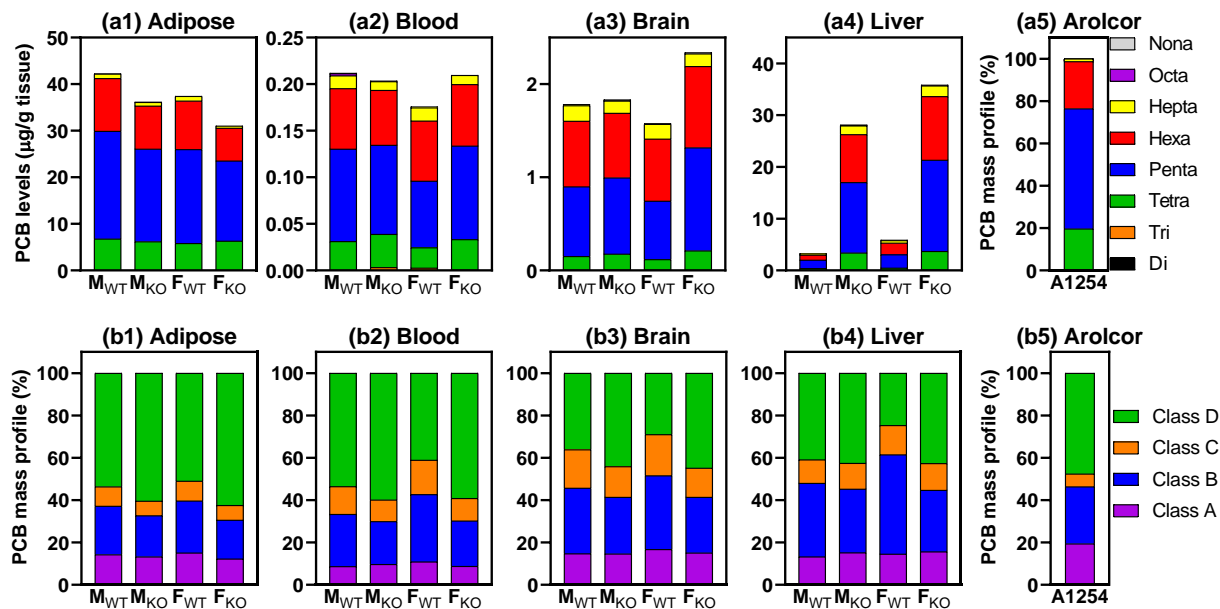
610 62. Pessah, I. N.; Lein, P. J.; Seegal, R. F.; Sagiv, S. K., Neurotoxicity of polychlorinated
611 biphenyls and related organohalogens. *Acta Neuropathol.* **2019**, *138*, 363-387.

612 63. Wayman, G. A.; Yang, D.; Bose, D. D.; Lesiak, A.; Ledoux, V.; Bruun, D.; Pessah, I. N.;
613 Lein, P. J., PCB-95 promotes dendritic growth via ryanodine receptor-dependent
614 mechanisms. *Environ. Health Perspect.* **2012**, *120*, 997-1002.

- 615 64. Wu, X.; Duffel, M.; Lehmler, H.-J., Oxidation of polychlorinated biphenyls by liver
616 tissue slices from phenobarbital-pretreated mice is congener-specific and atropselective.
617 *Chem. Res. Toxicol.* **2013**, *26*, 1642-1651.
- 618 65. Renaud, H. J.; Cui, J. Y.; Khan, M.; Klaassen, C. D., Tissue distribution and gender-
619 divergent expression of 78 cytochrome P450 mRNAs in mice. *Toxicol. Sci.* **2011**, *124*,
620 261-277.
- 621 66. Wu, X.; Kania-Korwel, I.; Chen, H.; Stamou, M.; Dammanahalli, K. J.; Duffel, M.; Lein,
622 P. J.; Lehmler, H.-J., Metabolism of 2,2',3,3',6,6'-hexachlorobiphenyl (PCB 136)
623 atropisomers in tissue slices from phenobarbital or dexamethasone-induced rats is sex-
624 dependent. *Xenobiotica* **2013**, *43*, 933-947.
- 625 67. Kania-Korwel, I.; Lukasiewicz, T.; Barnhart, C. D.; Stamou, M.; Chung, H.; Kelly, K.
626 M.; Bandiera, S.; Lein, P. J.; Lehmler, H.-J., Congener-specific disposition of chiral
627 polychlorinated biphenyls in lactating mice and their offspring: Implications for PCB
628 developmental neurotoxicity. *Toxicol. Sci.* **2017**, *158*, 101-115.
- 629 68. Dziennis, S.; Yang, D.; Cheng, J.; Anderson, K. A.; Alkayed, N. J.; Hurn, P. D.; Lein, P.
630 J., Developmental exposure to polychlorinated biphenyls influences stroke outcome in
631 adult rats. *Environ. Health Perspect.* **2008**, *116*, 474-480.
- 632 69. Miller, V. M.; Kahnke, T.; Neu, N.; Sanchez-Morrissey, S. R.; Brosch, K.; Kelsey, K.;
633 Seegal, R. F., Developmental PCB exposure induces hypothyroxinemia and sex-specific
634 effects on cerebellum glial protein levels in rats. *Int. J. Dev. Neurosci.* **2010**, *28*, 553-560.
- 635 70. Kodavanti, P. R. S.; Ward, T. R.; Derr-Yellin, E. C.; Mundy, W. R.; Casey, A. C.; Bush,
636 B.; Tilson, H. A., Congener-specific distribution of polychlorinated biphenyls in brain

- 637 regions, blood, liver, and fat of adult rats following repeated exposure to Arcolor 1254.
638 *Toxicol. Appl. Pharmacol.* **1998**, *153*, 199-210.
- 639 71. Wolff, M. S.; Thornton, J.; Fischbein, A.; Lilis, R.; Selikoff, I. J., Disposition of
640 polychlorinated biphenyl congeners in occupationally exposed persons. *Toxicol. Appl.*
641 *Pharmacol.* **1982**, *62*, 294-306.
- 642 72. Parham, F. M.; Kohn, M. C.; Matthews, H. B.; DeRosa, C.; Portier, C. J., Using structural
643 information to create physiologically based pharmacokinetic models for all
644 polychlorinated biphenyls. I. Tissue: blood partition coefficients. *Toxicol. Appl.*
645 *Pharmacol.* **1997**, *144*, 340-347.
- 646 73. Whitcomb, B. W.; Schisterman, E. F.; Buck, G. M.; Weiner, J. M.; Greizerstein, H.;
647 Kostyniak, P. J., Relative concentrations of organochlorines in adipose tissue and serum
648 among reproductive age women. *Environmental Toxicology and Pharmacology* **2005**, *19*,
649 203-213.
- 650 74. Artacho-Cordón, F.; Fernández-Rodríguez, M.; Garde, C.; Salamanca, E.; Iribarne-
651 Durán, L. M.; Torné, P.; Expósito, J.; Papay-Ramírez, L.; Fernández, M. F.; Olea, N.;
652 Arrebola, J. P., Serum and adipose tissue as matrices for assessment of exposure to
653 persistent organic pollutants in breast cancer patients. *Environ. Res.* **2015**, *142*, 633-643.
- 654 75. Ploteau, S.; Antignac, J.-P.; Volteau, C.; Marchand, P.; Vénisseau, A.; Vacher, V.; Le
655 Bizec, B., Distribution of persistent organic pollutants in serum, omental, and parietal
656 adipose tissue of French women with deep infiltrating endometriosis and circulating
657 versus stored ratio as new marker of exposure. *Environ. Int.* **2016**, *97*, 125-136.

- 658 76. Bachour, G.; Failing, K.; Georgii, S.; Elmadfa, I.; Brunn, H., Species and organ
659 dependence of PCB contamination in fish, foxes, roe deer, and humans. *Arch. Environ.*
660 *Contam. Toxicol.* **1998**, *35*, 666-673.
- 661 77. Lê Cao, K.-A.; Boitard, S.; Besse, P., Sparse PLS discriminant analysis: biologically
662 relevant feature selection and graphical displays for multiclass problems. *BMC*
663 *Bioinformatics* **2011**, *12*, 253.
- 664



665

666 **Fig 1.** Both the total PCB levels (Σ PCB) with homolog composition in (a1) adipose, (a2) blood, (a3) brain,

667 and (a4) liver and mass percentages based on PCB Class in (b1) adipose, (b2) blood, (b3) brain, (b4) liver

668 show genotype and sex-dependent differences. Levels of PCB congeners were measured by GC-MS in

669 tissues from male wildtype (M_{WT}), male knockout (M_{KO}), female wildtype (F_{WT}), and female knockout

670 (F_{KO}) mice exposed orally to Aroclor 1254. The composition of Aroclor 1254 by homolog group and Class

671 is shown for comparison in panels (a5) and (b5). Class A: PCBs congeners with a 4-, 3,4-, and 3,4,5-

672 substitution pattern and zero or one ortho chlorine substituent. Class B: PCB congeners with two or more

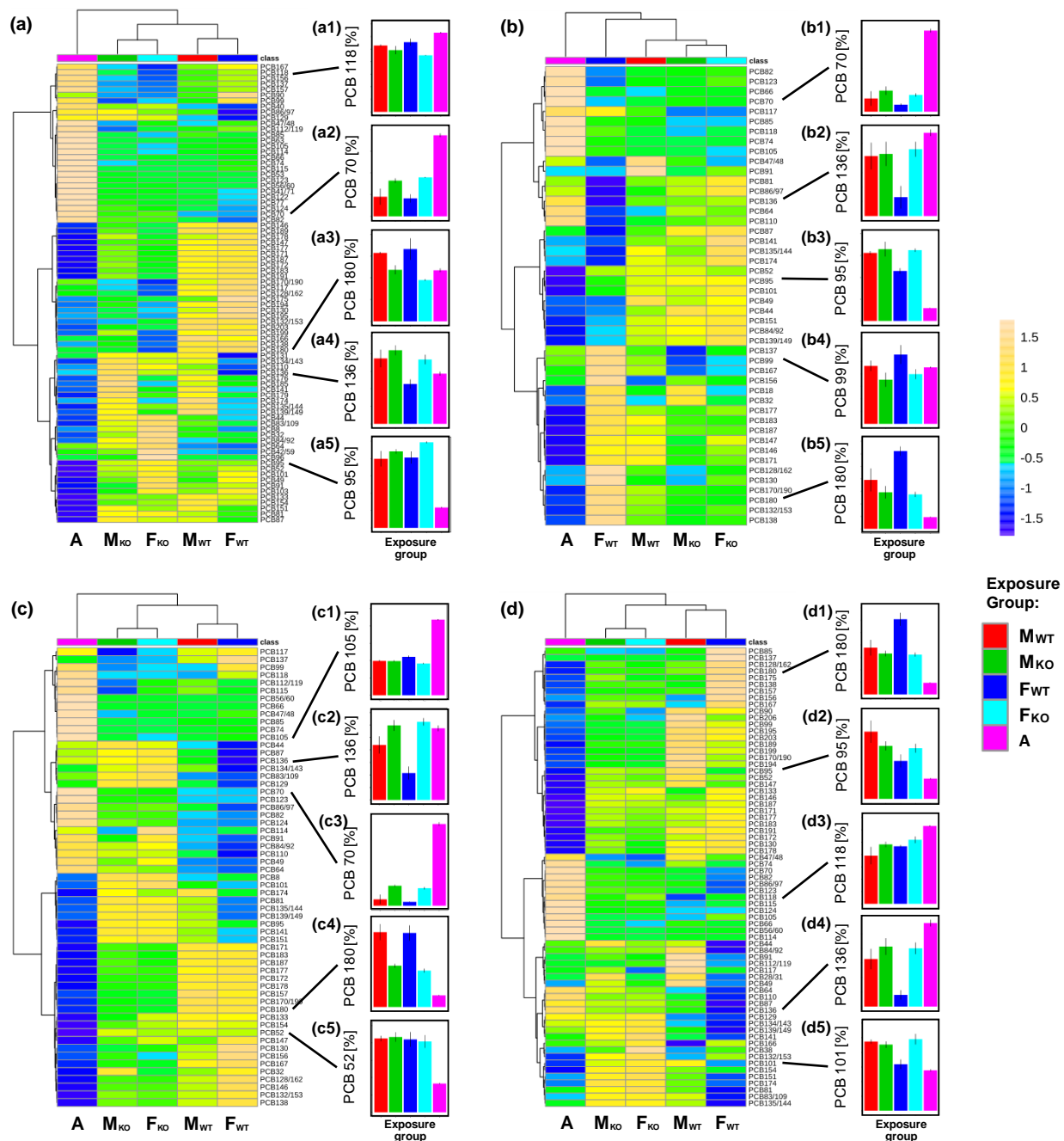
673 ortho chlorine substituents and a 2,4- or 2,3,4- substitution pattern. Class C: PCBs congeners with a 2,4,5-

674 substitution pattern. Class D: PCB congeners that, in contrast to Classes A through C, are readily

675 metabolized and, for example, have a 2-, 2,3-, 2,5- and 2,3,6-substitution pattern in at least one phenyl

676 ring.⁵⁰

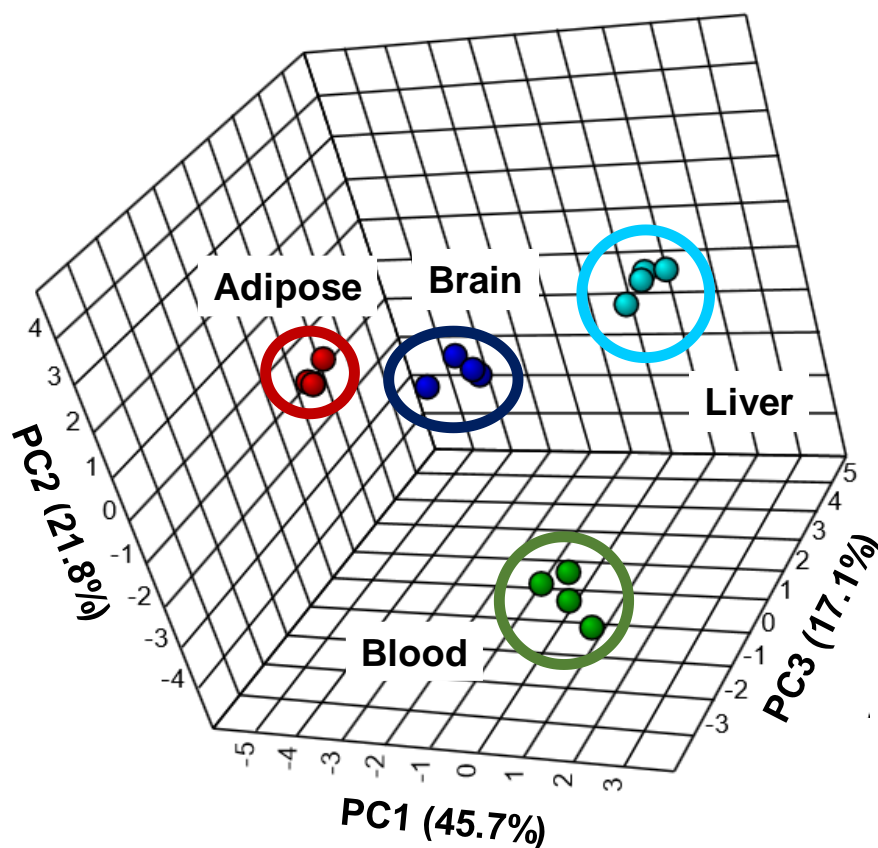
677



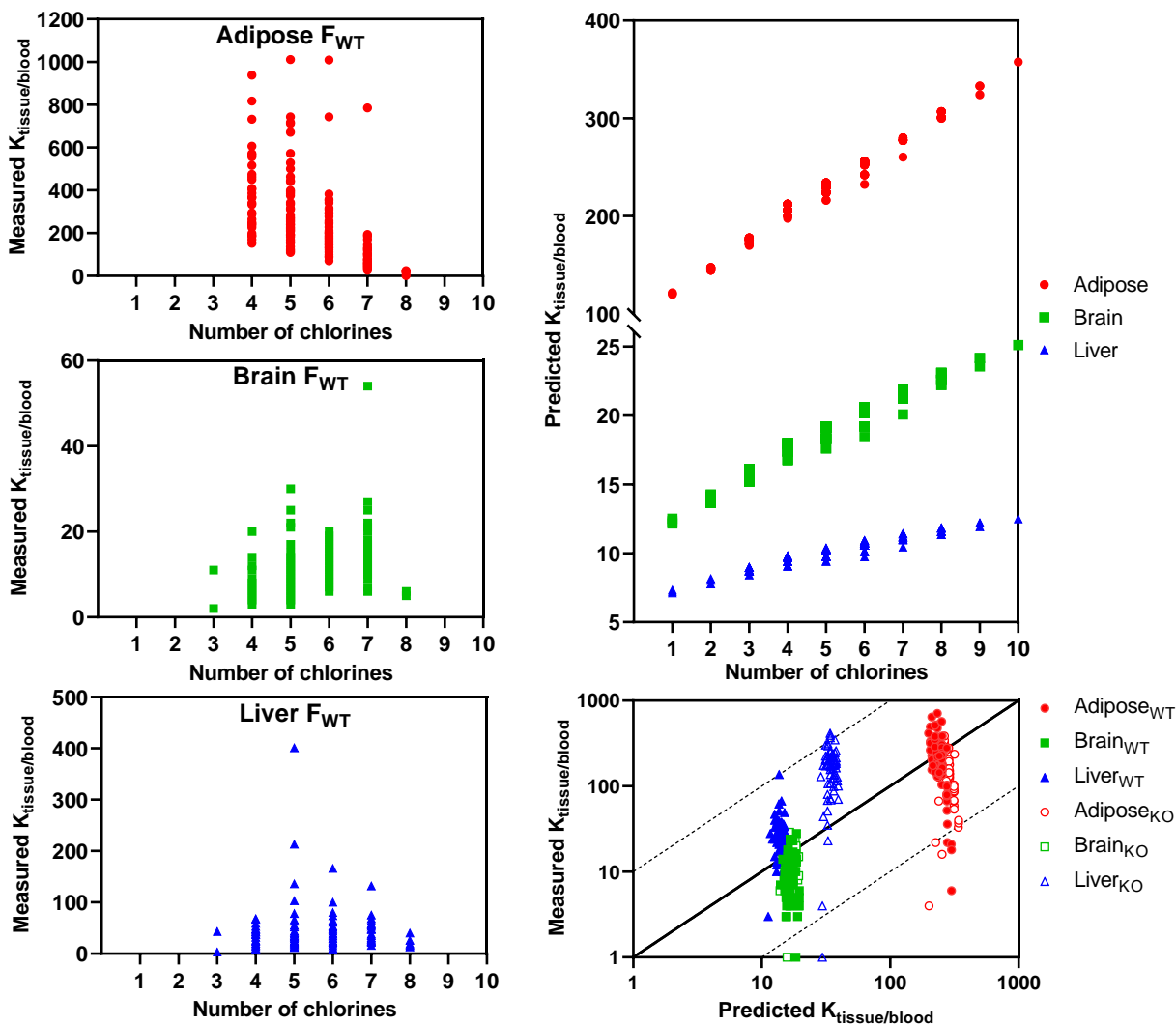
678

679 **Fig 2.** A comparison of the PCB congener profiles in (a) adipose tissue, (b) blood, (c) brain and (d) liver
 680 from male wildtype (M_{WT}), male knockout (M_{KO}), female wildtype (F_{WT}), and female knockout (F_{KO})
 681 mice reveals genotype-dependent differences in the distribution of individual PCB congeners in these
 682 tissues. The congener profile of Aroclor 1254 is shown for comparison. The small panels illustrate
 683 differences in the mass percentages of selected PCB congeners. Heatmaps were generated after removing

684 features with >25% missing values and autoscaling features of the original data using the Heatmap
685 function as implement by MetaboAnalyst 4.0.⁴⁰



686
 687 **Fig 3.** Sparse partial least squares - discriminant analysis (sPLS-DA)⁷⁷ revealed differences in the PCB
 688 congener profiles between tissues from F_{WT} mice (n = 4), with three principal components (PCs)
 689 accounting for 84.6% of the data variance. These differences were due to tissue-specific changes in the
 690 relative levels of PCB congeners that are more readily metabolized (Class D) vs. PCB congeners that are
 691 more resistant to metabolism (Classes A through C). PC1 separated adipose tissue from the brain and
 692 liver; PC2 separated blood from adipose tissue; PC3 separated the liver from other tissues. sPLS-DA was
 693 performed with PCB congener profiles using MetaboAnalyst 4.0 after removing variables for a threshold
 694 of 25%, cubic root transformation, and autoscaling features.⁴⁰ For analogous analyses of PCB congener
 695 profiles from M_{WT}, M_{KO}, and F_{KO} mice, see Figs. S8-S10 in the Supporting Information.



696
 697 **Fig 4.** Tissue : blood ratios ($K_{\text{tissue/blood}}$, (ng/g)/(ng/g)) of different PCB homolog groups in female wild
 698 type mice (F_{WT} , $n = 4$) show different trends with an increasing degree of chlorination: (a) Adipose : blood
 699 ratios decrease, (b) brain : blood ratios increase, and (c) liver : blood ratios of PCBs remain comparable
 700 with increasing degree of chlorination. Similar trends were observed with all other exposure groups
 701 (Figures S11-S13). (d) In contrast to the experimental findings, predicted tissue : blood ratios (i.e.,
 702 adipose : blood, brain : blood, and liver : blood ratios) increase with an increasing degree of chlorination.
 703 Data for the tissue composition were obtained from the literature.³³ (e) Despite this discrepancy, the
 704 predicted tissue : blood ratios are in reasonable agreement with the experimental values (for the

705 underlying tissue composition data, see Table S3). Each symbol represent the tissue : blood ratio of an
706 individual PCB congener.